Ubiquinone Binding Capacity of the *Rhodobacter capsulatus* Cytochrome bc_1 Complex: Effect of Diphenylamine, a Weak Binding Q_O Site Inhibitor†

R. Eryl Sharp,‡ Aimee Palmitessa,‡ Brian R. Gibney,‡ Jennifer L. White,‡ Christopher C. Moser,‡ Fevzi Daldal,§ and P. Leslie Dutton*,‡

Johnson Research Foundation, Department of Biochemistry and Biophysics, and Plant Science Institute, Department of Biology, University of Pennsylvania, Philadelphia, Pennsylvania 19104

Received November 5, 1998; Revised Manuscript Received January 25, 1999

ABSTRACT: Diphenylamine (DPA), a known inhibitor of polyene and isoprene biosynthesis, is shown to inhibit flash-activatable electron transfer in photosynthetic membranes of *Rhodobacter capsulatus*. DPA is specific to the Q_O site of ubihydroquinone:cytochrome *c* oxidoreductase, where it inhibits not only reduction of the $[2Fe\text{-}2S]^{2+}$ cluster in the FeS subunit and subsequent cytochrome *c* reduction but also heme b_L reduction in the cytochrome *b* subunit. In both cases, the kinetic inhibition constant (K_i) is 25 ± 10 μM. A novel aspect of the mode of action of DPA is that complete inhibition is established without disturbing the interaction between the reduced $[2Fe\text{-}2S]^{+}$ cluster and the Q_O site ubiquinone complement, as observed from the electron paramagnetic resonance (EPR) spectral line shape of the reduced [2Fe-2S] cluster, which remained characteristic of two ubiquinones being present. These observations imply that DPA is behaving as a noncompetitive inhibitor of the Q_O site. Nevertheless, at higher concentrations (>10 mM), DPA can interfere with the Q_O site ubiquinone occupancy, leading to a [2Fe-2S] cluster EPR spectrum characteristic of the presence of only one ubiquinone in the Q_O site. Evidently, DPA can displace the more weakly bound of the two ubiquinones in the site, but this is not requisite for its inhibiting action.

Ubihydroquinone:cytochrome *c* oxidoreductase (cyt[1] bc_1 complex in most organisms, cyt b_6f in chloroplasts) comprises the central portion of electron transfer chains in all energy-transducing organelles. The Q_O site is the locus of the primary energy conversion steps within the cyt bc_1 complex and initiates the conversion of the free energy between ubihydroquinone (QH_2) and ferricyt *c* into a transmembrane electrochemical gradient of protons. In prokaryotes, this site is located at the periplasmic face of the cytoplasmic membrane and in eukaryotes on the cytosolic side of the mitochondrial inner membrane (facing the intermembrane space). QH_2 oxidation is catalyzed by cooperation of two single-electron transfer chains which flank the Q_O site and transport the electrons in different directions. The redox cofactors closest to the site are the [2Fe-2S] cluster, the first cofactor in the high-potential chain which guides electrons to cyt c_1 and then to cytochromes *c* in the periplasm (or the mitochondrial intermembrane space); and cyt b_L, the first in the low-potential chain that through cyt b_H and the Q_i site drives electrons across the membrane to convert the redox potential differences into a transmembrane electrochemical gradient (*1*, *2*).

For one complete turnover of the cyt bc_1 complex to occur, two QH_2 molecules must be oxidized at the Q_O site (*3*, *4*). The conventional model depicts the Q_O site as binding one QH_2 at a time and performing two separate, serial oxidations. However, there is some controversy with regard to the Q_O site reaction dynamics, as well as the actual number of Q_O site ubiquinone occupants. The advent of crystal structures of cyt bc_1 complexes from various species with bound Q_O site specific inhibitors has assisted in defining the general Q_O site locality; however, in the native structures without inhibitors present, no electron density was identified that could be ascribed to ubiquinone (*5*−*8*). There are several plausible mechanisms for bifurcation of the electron transfer reaction in the Q_O site (*9*). These include (a) a double-Q occupancy model (*10*, *11*) invoking formation of a highly unstable ubisemiquinone transition state (*11*, *12*) or a quinhydrone-like intermediate (*11*, *13*); (b) a proton-gated charge transfer mechanism, where the activation barrier for the reaction is deprotonation of QH_2 (*14*, *15*); (c) a proton-gated affinity change mechanism implicating a stable ubisemiquinone intermediate (*7*, *16*); and (d) a model proposing formation of a single unstable ubisemiquinone diffusing within the Q_O site to facilitate bifurcated electron transfer by a catalytic switching movement (*7*, *12*, *13*). The recent structural demonstration that the [2Fe-2S] cluster moves over a distance of about 15 Å between the Q_O site and cyt c_1 adds another dynamic feature to the mechanisms for achieving efficient bifurcation of electron transfer (*5*−*8*).

† This work was supported by Public Health Service Grants GM 27309 to P.L.D. and GM 38237 to F.D.

* To whom correspondence should be addressed. Telephone: (215) 898-8699. Fax: (215) 898-0465. E-mail: dutton@mail.med.upenn.edu.

‡ Department of Biochemistry and Biophysics, University of Pennsylvania.

§ Department of Biology, University of Pennsylvania.

[1] Abbreviations: cyt, cytochrome; cyt b_L, low-potential cytochrome *b*; cyt b_H, high-potential cytochrome *b*; DPA, diphenylamine; EPR, electron paramagentic resonance; [2Fe-2S], iron−sulfur cluster of the FeS protein; MOA, methoxyacrylate; Q, ubiquinone; QH_2, ubihydroquinone; UHDBT, 5-undecyl-6-hydroxy-4,7-dioxobenzothiazole.

10.1021/bi982639+ CCC: $18.00
Published on Web 02/25/1999

A crucial aid in defining the function of the cyt bc_1 complex has been the use of specific, tight binding inhibitors, classified according to whether they affect catalysis at the Q_O or Q_i site (*17*). Another essential part of the progress into the Q_O site character has been provided by the electron paramagnetic resonance (EPR) spectral line shape of the reduced, paramagnetic [2Fe-2S] cluster. This has proven to be highly sensitive to the degree and nature of the Q_O site occupants (Q/QH_2 or inhibitors) (*10, 11*). Dutton and coworkers have proposed a working model, based on Q_O site occupancy and kinetic analysis of wild-type and mutant cyt bc_1 complexes, that is entirely consistent with the basic precedents of the Q-cycle hypothesis (*10, 11*). These studies indicated that the Q_O site is able to accommodate two ubiquinone molecules within two distinct binding domains, one of which was determined to have a high affinity and the other a lower affinity for Q/QH_2 and were accordingly designated the Q_{OS} (strong) and Q_{OW} (weak) domains, respectively. On the basis of this, a plausible model for one complete turnover of the cyt bc_1 complex was presented which only required exchange of ubiquinone in the Q_{OW} domain with the Q_{pool}.

Diphenylamine (DPA) is a well-known inhibitor of carotenoid (*18, 19*) and ubiquinone (*20*) synthesis whose action is clearly observed during the growth of photosynthetic prokaryotes. It has also been demonstrated that DPA can act as an inhibitor of the cyt bc_1 complex in vitro (*21*), as well as an effective inhibitor of photosystem II, but not photosystem I in chloroplasts (*22*). This report focuses on the nature of DPA inhibition of the cyt bc_1 complex in cytoplasmic membranes of the photosynthetic prokaryote *Rhodobacter capsulatus*. We show that DPA is most likely acting as a noncompetitive inhibitor of the Q_O site and discuss how the inhibiting action lends support to the double-occupancy mechanism.

EXPERIMENTAL PROCEDURES

Chromatophore preparation and extraction of ubiquinone from lyophilized chromatophores using isooctane were performed as previously described (*10*).

EPR measurements were performed on a Bruker ESP300E spectrometer (*23*). Temperature control was maintained by an Oxford ESR model 900 continuous flow cryostat interfaced with an Oxford model ITC4 temperature controller. The frequency was measured by a Hewlett-Packard model 5350B frequency counter. Typical operating parameters were as follows: sample temperature, 20 K; microwave frequency, 9.474 GHz; microwave power, 2 mW; modulation frequency, 100 kHz; modulation amplitude, 19.8 G; and time constant, 164 ms. Sample concentrations were typically 10 μM reaction center. Further specific experimental details are provided in the figure legends.

Flash-activated turnover of the cyt bc_1 complex was performed on a Biomedical Johnson Foundation single-wavelength spectrophotometer (University of Pennsylvania) fitted with an anaerobic redox cuvette as previously described (*23*).

All chemicals were purchased from Aldrich Chemical Co. (Milwaukee, WI), except for the cyt bc_1 inhibitors stigmatellin and antimycin, which were purchased from Sigma Chemical Co. (St. Louis, MO). All mediators and inhibitors were added as solutions in dimethyl sulfoxide; at the concentrations used, this solvent has no effect upon the cyt bc_1 complex kinetic activity or the [2Fe-2S] cluster EPR spectrum (*10*).

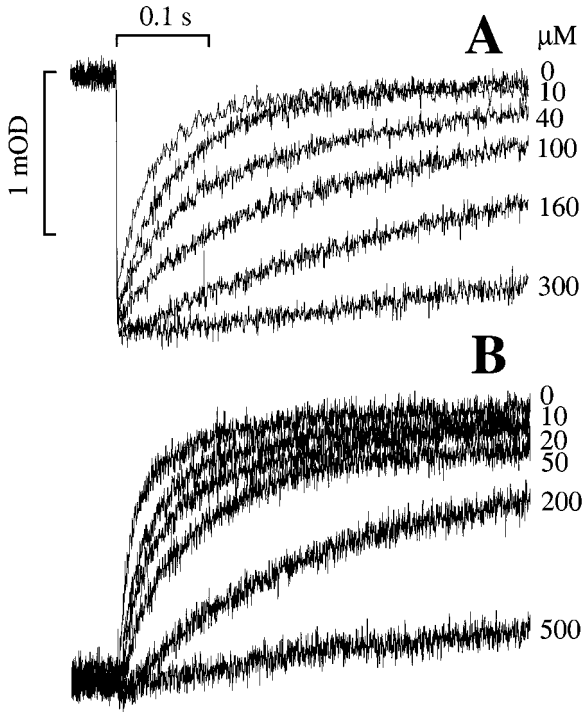

FIGURE 1: Effect of diphenylamine (DPA) upon the cyt bc_1 complex Q_O site function with the Q_{pool} fully oxidized. The chromatophores were suspended to a reaction center concentration of 0.2 μM and poised at a redox potential of 200 mV to establish the fully oxidized Q_{pool}. Valinomycin (5 μM) was added as an uncoupler. (A) Flash-activated total cyt *c* absorption changes (550−540 nm) in the absence of antimycin, illustrating the inhibition of cyt *c* re-reduction by increasing concentrations of DPA. The numbers beside the traces denote the DPA concentration in micromolar. (B) Flash-activated cyt *b* absorption changes (560−570 nm) obtained under conditions identical to those described for panel A, except 10 μM antimycin was added to inhibit cyt *b* reoxidation by the Q cycle. The dynamics of the flash-induced absorption changes of cytochromes *b* and *c* were best described by biphasic exponential decays (data not shown). Each trace is the sum of 20 individual flashes. Sufficient time was allowed between each flash for the system to return to equilibrium.

RESULTS

Inhibition of Q_O Site Function by DPA with the Q_{pool} Fully Oxidized Prior to Activation. When the Q_{pool} is fully oxidized prior to flash activation, the Q_O site contains only oxidized ubiquinone (Q) at the time of activation and the substrate QH_2 is provided by the Q_B site of the photosynthetic reaction center. Under these conditions, the QH_2 released from the Q_B site must diffuse to the Q_O site and displace the resident Q prior to being oxidized itself. Figure 1 shows the effect of DPA upon the kinetics of the cyt bc_1 complex, where incremental additions of DPA exert a parallel effect upon the re-reduction of cytochromes *c* and the reduction of cyt b_H. In both cases, DPA decreases the rate constants but not the overall amplitude of the reduction (cyt *b*) or re-reduction (cytochromes *c*) processes, respectively. These observations imply that DPA appears to be behaving as a typical competitive inhibitor of the Q_O site. Figure 2 shows the inhibition profile of DPA fitted to a simple inhibition

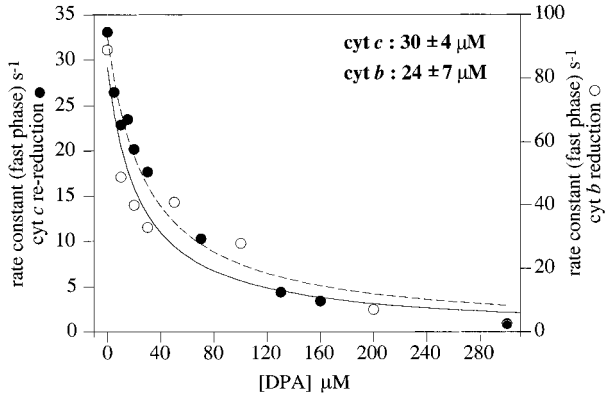

FIGURE 2: Illustration of the cyt bc_1 complex Q_O site inhibition by DPA when the Q_{pool} is fully oxidized. The rate constants for reduction of cytochromes *b* and *c* were obtained from the dominant fast phase of biphasic exponential fits to the experimental traces shown in Figure 1. The data were fit to a simple inhibition equation (dashed line, cytochrome *c*; solid line, cyt *b*): $k_{obs} = k_O/[1 + ([DPA]/K_i)]$, where k_{obs} is the measured rate constant (s^{-1}), k_O is the rate constant in the absence of inhibitor (s^{-1}), [DPA] is the concentration of added DPA (M), and K_i is the concentration of DPA required to produce 50% inhibition (M). The K_i values obtained from the data for cytochromes *b* and *c* are indicated in the figure.

equation for both the cyt *b* and *c* reduction data when the Q_{pool} is fully oxidized prior to flash activation. It is clear that DPA inhibits cyt *b* reduction and cyt *c* re-reduction in the same fashion, and the inhibition constants (K_i) are identical within experimental error (25 ± 10 μM).

Inhibition of Q_O Site Function by DPA with QH_2 in the Q_{pool} Prior to Activation. Figure 3 shows the effect of DPA upon the kinetics of the cyt bc_1 complex when the Q_{pool} is half-reduced. In this case, upon flash activation, QH_2 either is initially present in the Q_O site or is derived directly from the Q_{pool}; hence, the overall kinetics are faster than those requiring diffusion of QH_2 generated at the Q_B site, as described above. Figure 3A illustrates the behavior of the total cyt *c* re-reduction kinetics under multiple flash turnover conditions. From a comparison of the kinetic traces presented in Figures 1 and 3, it is apparent that the inhibition of cytochromes *b* and *c* follows the same pattern and is independent of the Q_{pool} redox state. This observation is confirmed in Figure 4, where the inhibition profile of DPA is fitted to the inhibition equation for both cyt *b* reduction and cyt *c* re-reduction when the Q_{pool} is half-reduced prior to flash activation. The value of K_i for both cytochromes *b* and *c* is the same within experimental error as that obtained when the Q_{pool} is fully oxidized (Figures 2 and 4).

Evidence for Specific Inhibition of the Q_O Site by DPA. It is clear from the total cyt *c* re-reduction traces presented in Figure 3A that DPA inhibition over the concentration range investigated is manifested at the level of the Q_O site and not at the Q_A or Q_B site of the reaction center. Protocols facilitating a closer examination of the inhibition at the Q_B site are well-established (*24*, *25*). If DPA had affected the function of the Q_A or Q_B site, then upon addition of increasing amounts of DPA under multiple saturating flash turnover of the reaction center (as is occurring in Figure 3A), the amplitude of the total cyt *c* oxidation signal with successive light flashes would dramatically decrease, which is clearly not the case. Analysis of the rate constants for charge recombination to the bacteriochlorophyll special pair

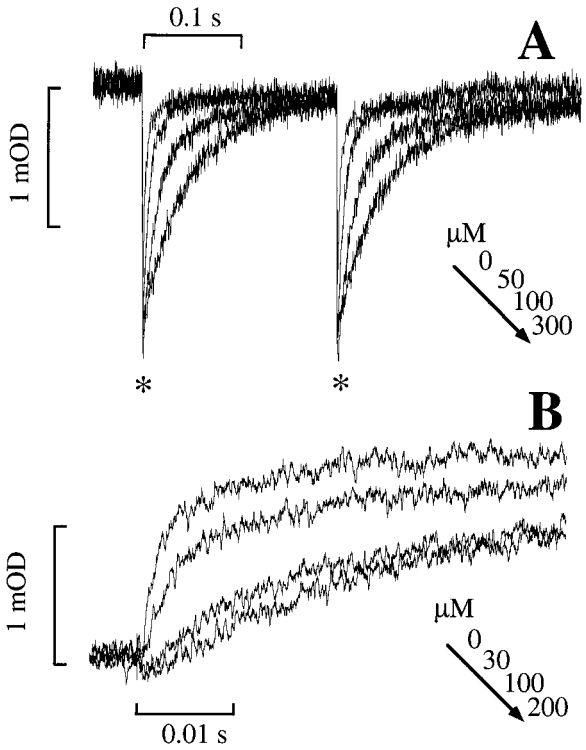

FIGURE 3: Effect of DPA upon cyt bc_1 complex Q_O site function with ubihydroquinone (QH_2) present in the Q_{pool}. Initial experimental conditions were exactly as described for Figure 1, except the redox potential was poised at 100 mV under which conditions the Q_{pool} comprises an equal amount of QH_2 and Q. (A) Flash-activated total cyt *c* absorption changes (550−540 nm) in the absence of antimycin, illustrating the inhibition of cytochrome *c* re-reduction by increasing amounts of DPA. The sample was subjected to two successive exciting light flashes 0.2 s apart, indicated on the figure with asterisks. The numbers beside the traces denote the DPA concentration in micromolar. (B) Flash-activated cyt *b* absorption changes (560−570 nm) obtained under conditions identical to those described for panel A, except 10 μM antimycin was added to inhibit cyt *b* reoxidation by the Q cycle and only one exciting flash per cycle was delivered. The dynamics of the flash-induced absorption changes of cytochromes *b* and *c* were best described by monophasic and biphasic exponential decays, respectively (data not shown).

(P^+) provides direct information with regard to the reaction center Q_B site occupancy by ubiquinone. The charge recombination is more rapid when the Q_B site is inhibited, since the process occurs directly from ubiquinone in the Q_A site (14.4 vs 0.9 s^{-1}) (*10*, *26*). Addition of 1 mM DPA has no effect on the charge recombination kinetics, providing further evidence that DPA does not inhibit Q_B site function (data not shown). Examination of the inhibition of the cyt bc_1 complex Q_i site was also followed by established methodology based on the reverse electron transfer reaction from QH_2 to cyt b_H at pH 9.0, where this process becomes thermodynamically favorable (*27*). There was no evidence for DPA inhibiting the cyt bc_1 complex Q_i site over the same concentration range as the Q_O site (up to 1 mM DPA, data not shown). Thus, even though DPA is a weak binding inhibitor of the cyt bc_1 complex, its inhibitory action is specific to the Q_O site.

EPR Spectral Changes of the [2Fe-2S] Cluster Induced by Inhibiting Amounts of DPA. Figure 5 shows the concentration dependence of the DPA effect upon the EPR spectral line shape of the [2Fe-2S] cluster. In the absence of DPA,

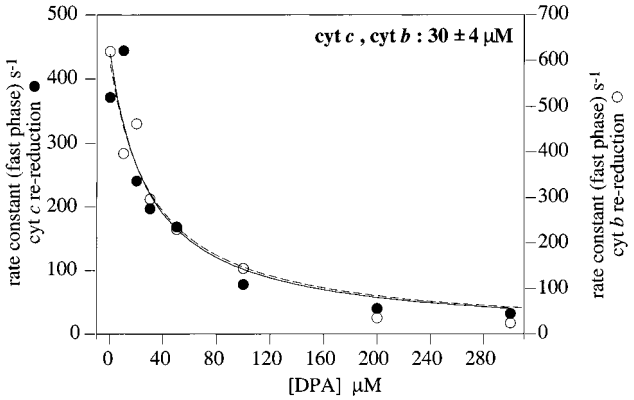

FIGURE 4: Illustration of the cyt bc_1 complex Q_O site inhibition by DPA with 50% QH_2 present in the Q_{pool}. The rate constants for reduction of cytochromes *b* and *c* were obtained from the monophasic and the dominant fast phase of biphasic exponential fits, respectively, of the experimental traces shown in Figure 3. The data are fit to the same equation described in the legend of Figure 2 (dashed line, cyt *c*; solid line, cyt *b*). The values for K_i obtained from the data for cytochromes *c* and *b* are indicated in the figure.

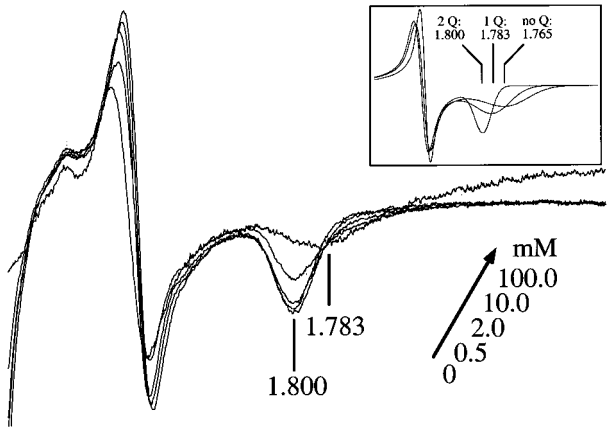

FIGURE 5: Titration of the DPA-induced cyt bc_1 complex [2Fe-2S] cluster EPR spectrum in chromatophores containing wild-type levels of ubiquinone. All samples were suspended to a reaction center concentration of 10 μM and poised at 200 mV. Each spectrum is a sum of five successive scans. The numbers refer to the concentration of added DPA, resulting in the loss of the g_x resonance at 1.800 and the appearance of the g_x signal at 1.783 upon saturation with DPA. The inset shows simulations of typical [2Fe-2S] cluster EPR spectra with various ubiquinone Q_O site occupancies, as obtained with the Q_{pool} oxidized and the [2Fe-2S] cluster reduced, generated using the program EPRSim XOP for Igor Pro (J. Boswell, Oregon Graduate Institute, Beaverton, OR).

the [2Fe-2S] cluster EPR line shape is characteristic of the native Q_O site fully occupied by ubiquinone with a g_x resonance at 1.800. Significantly, there is no detectable change in the [2Fe-2S] EPR spectrum at DPA concentrations which completely inhibit the Q_O site kinetics (20-fold higher than the K_i value). However, the [2Fe-2S] cluster EPR spectral line shape induced by higher concentrations of DPA (>10 mM) is very similar to that obtained for Q-extracted chromatophore membranes, when there is only one Q present in the Q_{OS} domain of the Q_O site (*10*). In both cases, the line shape and position of the g_x resonance are the same and are at a value of 1.783. There are two possible explanations for this. (a) At high concentrations, the DPA-induced EPR spectral change could be due to DPA itself interacting directly with the [2Fe-2S] cluster and coincidentally yielding the same line shape. (b) Alternatively, DPA binding in the

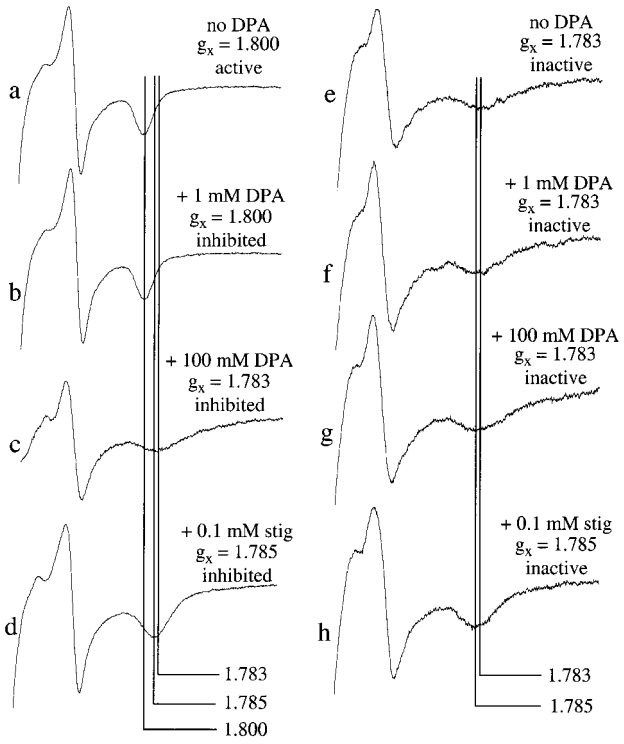

FIGURE 6: Comparison of the effect of DPA upon the cyt bc_1 complex [2Fe-2S] cluster EPR spectrum in chromatophores containing wild-type levels of ubiquinone (a−d) and partially extracted ubiquinone, such that only the Q_{OS} domain of the Q_O site is occupied (e−h). Sample preparation and EPR conditions were as described in the legend of Figure 5. Spectra a and e are typical for two ubiquinone molecules in the Q_O site (g_x resonance at 1.800) and one ubiquinone molecule in the Q_{OS} domain of the Q_O site (g_x resonance at 1.783), respectively. The effects on the EPR spectra are shown for successive additions of 1 mM DPA (b and f), 100 mM DPA (c and g), and 0.1 mM stigmatellin (d and h).

Q_O site and displacing Q from the Q_{OW} domain results in an EPR spectral line shape reporting the occupancy of only the Q_{OS} domain by Q. One line of evidence that DPA does not interact directly with the [2Fe-2S] cluster, even at high concentrations, is that in extensively Q-extracted chromatophores (such that the Q_O site is devoid of Q), no change occurs in the EPR spectral line shape of the [2Fe-2S] cluster (g_x resonance at 1.765), even at 100 mM DPA. Furthermore, as shown in Figure 6, addition of up to 100 mM DPA has no effect on the [2Fe-2S] cluster EPR spectral line shape in partially Q-extracted chromatophores, such that only the Q_{OS} domain of the Q_O site is occupied by Q (g_x resonance at 1.783), thus demonstrating that DPA does not mimic the EPR effect of Q in the Q_{OW} domain. In light of this result, it seems clear that explanation (b) is correct. Although DPA appears to displace Q from the Q_{OW} domain at high concentrations, it does not do so at sub-millimolar concentrations, since if this were to occur, the [2Fe-2S] cluster EPR spectral line shape would be indicative of one Q in the Q_{OS} domain of the Q_O site (g_x at 1.783), which is clearly not the case (Figure 6). Under all conditions, addition of the tight binding Q_O (at 0.1 mM) site specific inhibitor, stigmatellin to chromatophores produced the characteristic stigmatellin-induced [2Fe-2S] EPR spectral line shape with a prominent g_x resonance at 1.785 (*10*, *28*), implying that stigmatellin overrides the DPA effect, even in the presence of 100 mM DPA (Figure 6). The effect of high concentrations of DPA (>10 mM) upon the [2Fe-2S] cluster EPR spectral line shape is not

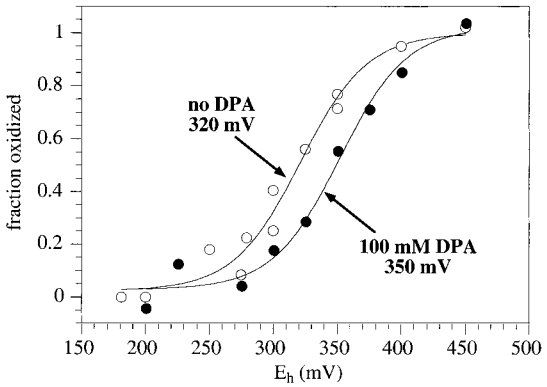

FIGURE 7: Redox midpoint potential of the cyt bc_1 complex [2Fe-2S] cluster in the absence (○) and presence of 100 μM DPA (●). The fraction reduced was determined from the peak to trough amplitude difference of the g_y resonance, and the data were fit to the Nernst equation for a one-electron couple, with the indicated midpoint potentials (standard error ± 10 mV). Chromatophores were suspended to a reaction center concentration of 10 μM, and the EPR conditions are as reported in Experimental Procedures.

directly relevant to the mechanism of Q_O site kinetic inhibition by DPA, since the concentration ranges over which these effects are manifested are well resolved from one another. Therefore, sub-millimolar concentrations of DPA can bind to the Q_O site and affect Q_O site function without disrupting the interaction of Q with the [2Fe-2S] cluster, implying that the Q_O site can accommodate a full complement of Q/QH_2 and also bind DPA. From these conclusions, it is apparent that DPA is not behaving as a typical competitive inhibitor, by displacing Q/QH_2 from the Q_O site, but rather more likely as a noncompetitive inhibitor.

Effect of DPA on the [2Fe-2S] Cluster Redox Midpoint Potential. The effect of saturating amounts of DPA (100 mM) on the cyt bc_1 complex [2Fe-2S] cluster redox midpoint potential is illustrated in Figure 7. The midpoint potential of the one-electron $[2Fe\text{-}2S]^{2+/+}$ couple is slightly elevated by about 30 mV in the presence of DPA (*28*). This implies that DPA binds with an about 5-fold greater affinity to the Q_O site of the cyt bc_1 complex when the [2Fe-2S] cluster is in the reduced state.

DISCUSSION

Mechanism of Q_O Site Inhibition by DPA. Figure 8 shows a schematic representation of DPA interacting with the Q_O site and depicts a possible mechanism for the inhibition process, based on the two-Q/QH_2 site model of Ding et al. (*10, 11*). In part A, the arrow indicates the rapid equilibrium for exchange of Q/QH_2 in the Q_{OW} domain of the Q_O site with the Q_{pool} (*10, 11*), with the rate of exchange governing the turnover kinetics of the cyt bc_1 complex. Part B illustrates the noncompetitive Q_O site inhibition exerted by sub-millimolar concentrations of DPA, where the interaction of Q/QH_2 in the Q_O site with the [2Fe-2S] cluster is not disrupted, but QH_2 oxidation is impeded by DPA binding at a tertiary position in or near the Q_O site. As yet, we are unsure of the actual physical mechanism for Q_O site inhibition by DPA; however, it cannot solely be due to DPA impeding exchange of Q/QH_2 in the Q_{OW} domain with the Q_{pool}, since the inhibition kinetics are independent of the oxidation state of ubiquinone in the Q_O site. Part C shows displacement of Q/QH_2 in the Q_{OW} domain by high concentrations of DPA, where the [2Fe-2S] cluster EPR spectral line shape reports the occupancy of the Q_{OS} domain by Q/QH_2 and an empty Q_{OW} domain. It should be noted from the data summarized in Figure 7 that the model of DPA inhibition is also compatible with a high degree of plasticity with respect to the number of Q/QH_2 occupants of the Q_{OW} domain within the Q_O site. In light of the obtained results, the most important point to arise from this report is that the effect of DPA upon Q_O site catalysis is quite readily explained in terms of the double-occupancy model as originally proposed by Ding et al. (*10*).

Comparison of Q_O Site Inhibition by DPA with Other Inhibitors. Q_O site specific cyt bc_1 complex inhibitors have been conveniently grouped according to their inhibiting action (*17*). Group I includes the β-methoxyacrylates, for

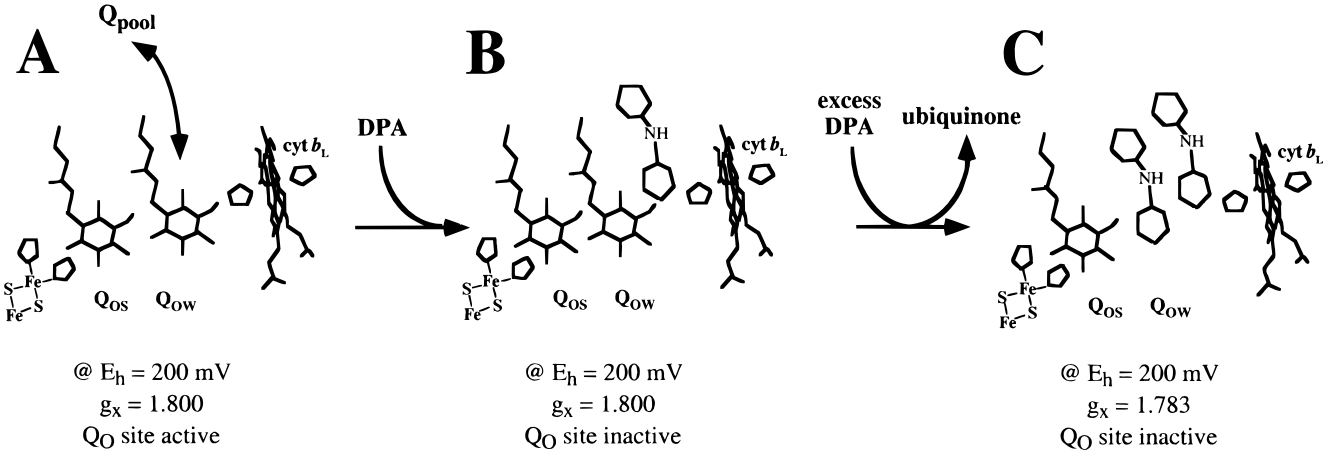

FIGURE 8: Schematic representation of the cyt bc_1 complex depicting the effect of DPA on the ubiquinone binding capacity of the Q_O site. The Q_O site is flanked by the [2Fe-2S] cluster of the FeS subunit and heme b_L of the cyt *b* subunit (also shown are the liganding histidine imidazole groups). (A) Two Q molecules bound at the Q_O site, producing the characteristic reduced [2Fe-2S] cluster EPR spectrum with a prominent g_x signal at 1.800. (B) Upon addition of DPA (≤1.0 mM), no change in the [2Fe-2S] EPR spectral line shape occurs, but Q_O site catalysis is inhibited, presumably by noncompetitive inhibition. (C) When excess DPA is added (>10 mM) to the inhibited cyt bc_1 complex, the [2Fe-2S] cluster EPR spectral line shape changes, with the prominent g_x at 1.800 being replaced by a shallower feature at 1.783. This is depicted as being due to displacement of Q in the Q_{OW} domain by DPA. It should be noted that DPA inhibits electron transfer to the [2Fe-2S] cluster and cyt b_L, and the fact that the figure shows DPA binding proximal to the b_L heme does not indicate that only cyt b_L heme reduction is inhibited. The figure is discussed in the text.

example, myxothiazol (*29*) and methoxy-acrylate-stilbene (*30*−*33*), which typically bind with sub-nanomolar dissociation constants and inhibit electron transfer from QH_2 to the [2Fe-2S] cluster of the FeS subunit and onto cyt b_L but, in the case of myxothiazol at least, do not inhibit reduction of cytochromes *c* by the [2Fe-2S] cluster (not yet determined for MOA-stilbene). Group II includes the hydroxyquinone analogues, for example, 5-undecyl-6-hydroxy-4,7-dioxobenzothiazole (UHDBT) (*34*) and 3-alkyl-2-hydroxy-1,4-naphthoquinones (alkyl HNQ) (*35*), which bind with a lower affinity than the group I inhibitors and specifically affect the properties of the [2Fe-2S] cluster but not cyt b_L. They act by inhibiting electron transfer from the [2Fe-2S] cluster to cyt c_1, as well as onto cyt b_L. The chromone inhibitors typified by stigmatellin exhibit properties of both group I and II inhibitors, binding tightly with sub-nanomolar K_d values and inhibiting electron transfer from QH_2 to the [2Fe-2S] cluster and cyt b_L, and [2Fe-2S] to cyt c_1 (*36*). From the properties of DPA presented in this paper, it is clear that this inhibitor cannot be exclusively classified into any one of these classic groups since it appears to have properties in common with several of the above-mentioned inhibitors from different groups, as well as possessing unique inhibiting characteristics of its own. Like DPA, MOA-stilbene also has been shown to bind noncompetitively to the Q_O site of the mitochondrial cyt bc_1 complex (*30*). Moreover, it is interesting to note that when the complex is fully reduced, two MOA-stilbene molecules are able to bind to the Q_O site. However, the Q/QH_2 occupancy of the Q_O site was not determined under these conditions, and the identity of the cofactor whose reduction controls this binding change is currently unknown (*33*). It is not yet established whether binding of one or two MOA-stilbene molecules at the Q_O site affects the [2Fe-2S] cluster EPR spectral properties; this is presently under investigation (R. E. Sharp and P. L. Dutton, experiments in progress).

Comparison of cyt bc_1 Complex Inhibition by DPA with the Effect of Q_O Site Mutations. Site-directed mutations of Y147 → S/A in the cyt *b* subunit of the *R. capsulatus* cyt bc_1 complex severely disrupt Q_O site catalysis, but from the appearance of the [2Fe-2S] cluster EPR spectral line shape, they do not induce loss of ubiquinone from the Q_O site (*37*). The effect of these mutations appears to be very similar to that of DPA described in this paper. Electron transfer from QH_2 in the Q_O site to the [2Fe-2S] cluster and cyt b_L is impeded by these mutations. In the cyt bc_1 complex crystal structures, Y147 is located close to heme b_L and at one end of the presumed Q_O site (*5*−*8*). The effect of the mutations was interpreted as a strict requirement for tight side chain packing and a high degree of hydrophobicity in establishing efficient electron transfer from QH_2 to the [2Fe-2S] cluster and cyt b_L (*37*). In light of these findings, we suggest that DPA may inhibit by binding in the vicinity of Y147 and perhaps disrupt the protein packing, hindering efficient QH_2 oxidation in the Q_O site.

ACKNOWLEDGMENT

We thank Dr. E. A. Berry for making available structural data of higher eukaryotic cyt bc_1 complexes from various species.

REFERENCES

1. Brandt, U., and Trumpower, B. L. (1994) *Crit. Rev. Biochem. Mol. Biol. 29*, 165−197.
2. Gray, K. A., and Daldal, F. (1995) in *Anoxygenic Photosynthetic Bacteria* (Blankenship, R. E., Madigan, M. T., and Bauer, C., Eds.) pp 725−745, Kluwer Academic Publishers, Dordrecht, The Netherlands.
3. Lawford, H. G., and Garland, P. B. (1983) *Biochem. J. 130*, 1029−1044.
4. Crofts, A. R., and Wraight, C. A. (1983) *Biochim. Biophys. Acta 726*, 149−185.
5. Xia, D., Yu, C.-A., Kim, H., Xia, J.-Z., Kachurin, A. M., Zhang, L., Yu, L., and Deisenhofer, J. (1997) *Science 277*, 60−66.
6. Zang, Z., Huang, L., Shulmeister, M. L., Chi, Y.-I., Kim, K. K., Hung, L.-W., Crofts, A. R., Berry, E. A., and Kim, S.-H. (1998) *Nature 392*, 677−684.
7. Iwata, S., Lee, J. W., Okada, K., Lee, J. K., Iwata, M., Rasmussen, B., Link, T. A., Ramaswamy, S., and Jap, B. K. (1998) *Science 281*, 64−71.
8. Kim, H., Xia, D., Yu, C.-A., Xia, J.-Z., Kachurin, A. M., Zhang, L., Yu, L., and Deisenhofer, J. (1998) *Proc. Natl. Acad. Sci. U.S.A. 95*, 8026−8033.
9. Junemann, S., Heathcote, P., and Rich, P. R. (1998) *J. Biol. Chem. 273*, 21603−21607.
10. Ding, H., Robertson, D. E., Daldal, F., and Dutton, P. L. (1992) *Biochemistry 31*, 3144−3158.
11. Ding, H., Moser, C. M., Robertson, D. E., Tokito, M. K., Daldal, F., and Dutton, P. L. (1995) *Biochemistry 34*, 15979−15996.
12. Crofts, A. R., Barquera, B., Gennis, R. B., Kuras, R., Guergova-Kuras, M., and Berry, E. A. (1997) in *The Photrophic Prokaryotes* (Peschek, G. A., Loffelhard, W., and Schmetterer, G., Eds.) Plenum Publishing Corp., New York (in press).
13. Crofts, A. R., and Wang, Z. (1989) *Photosynth. Res. 22*, 69−87.
14. Brandt, U. (1996) *FEBS Lett. 387*, 1−6.
15. Brandt, U., and Okun, J. G. (1997) *Biochemistry 36*, 11234−11240.
16. Link, T. A. (1997) *FEBS Lett. 412*, 257−264.
17. von Jagow, G., and Link, T. A. (1986) *Methods Enzymol. 126*, 253−271.
18. Goodwin, T. W., and Osman, H. G. (1954) *Biochem. J. 56*, 222−230.
19. Turner, J. A., and Prebble, J. N. (1980) *J. Gen. Microbiol. 119*, 133−144.
20. Sugimura, T., and Rudney, H. (1962) *Biochim. Biophys. Acta 62*, 167−170.
21. Bashford, C. L., Prince, R. C., Takamiya, K.-I., and Dutton, P. L. (1979) *Biochim. Biophys. Acta 545*, 223−235.
22. Oettmeier, W., and Renger, G. (1980) *Biochim. Biophys. Acta 593*, 113−124.
23. Sharp, R. E., Palmitessa, A., Gibney, B. R., Moser, C. C., Daldal, F., and Dutton, P. L. (1997) in *The Photrophic Prokaryotes* (Peschek, G. A., Loffelhard, W., and Schmetterer, G., Eds.) Plenum Publishing Corp., New York (in press).
24. Giangiacomo, K. M., and Dutton, P. L. (1989) *Proc. Natl. Acad. Sci. U.S.A. 86*, 2658−2662.
25. Shopes, R. J., and Wraight, C. A. (1985) *Biochim. Biophys. Acta 806*, 348−356.
26. Okamura, M. Y., Iaacson, R. H., and Feher, G. (1975) *Proc. Natl. Acad. Sci. U.S.A. 72*, 3491−3495.
27. Robertson, D. E., Giangicomo, K. M., de Vries, S., Moser, C. C., and Dutton, P. L. (1984) *FEBS Lett. 178*, 343−350.
28. Sharp, R. E., Palmitessa, A., Gibney, B. R., Moser, C. C., Daldal, F., and Dutton, P. L. (1998) *FEBS Lett. 431*, 423−426.
29. von Jagow, G., Ljungdahl, P. O., Graf, P., Ohnishi, T., and Trumpower, B. L. (1984) *J. Biol. Chem. 259*, 6318−6326.
30. Brandt, U., Schägger, H., and von Jagow, G. (1988) *Eur. J. Biochem. 173*, 499−506.

31. Brandt, U., and von Jagow, G. (1991) *Eur. J. Biochem. 195*, 163−170.
32. Brandt, U., Haase, U., Schägger, H., and von Jagow, G. (1991) *J. Biol. Chem. 266*, 19958−19964.
33. Brandt, U., and Djafarzadeh-Andabili, R. (1997) *Biochim. Biophys. Acta 1321*, 238−242.
34. Bowyer, J. R., Edwards, C. A., Ohnishi, T., and Trumpower, B. L. (1982) *J. Biol. Chem. 257*, 8321−8330.
35. Matsuura, K., Bowyer, J., Ohnishi, T., and Dutton, P. L. (1983) *J. Biol. Chem. 258*, 1571−1579.
36. von Jagow, G., and Ohnishi, T. (1985) *FEBS Lett. 185*, 311−315.
37. Saribas, A. S., Ding, H., Dutton, P. L., and Daldal, F. (1995) *Biochemistry 34*, 16004−16012.

BI982639+